Poly(ethylene glycol) Gradient for Biochip Development

Andréas Larsson and Bo Liedberg*

Division of Sensor Science and Molecular Physics, Department of Physics, Chemistry and Biology, Linköping University, SE-581 83 Linköping, Sweden

Received March 13, 2007. In Final Form: July 18, 2007

A novel method of producing a poly(ethylene glycol) (PEG)-based gradient matrix that varies gradually in thickness from 0 to 500 Å over a distance of 5−20 mm is presented. The gradient matrix is graft copolymerized from a mixture of PEG methacrylates onto organic thin films providing free radical polymerization sites initiated by UV irradiation at 254 nm. The films used as grafting platforms consist of either a spin-coated cycloolefin polymer or a self-assembled monolayer on planar gold. The thickness/irradiation gradient is realized by means of a moving shutter that slowly uncovers the modified gold substrate. The structural and functional characteristics of the gradient matrix are investigated with respect to thickness profile, degree of carboxylation, and subsequent immobilization of two model proteins of different sizes and shapes. These characteristics are studied with ellipsometry and infrared reflection−absorption microscopy using a grazing angle objective. It is revealed that the relatively small carboxylation agent used offers homogeneous activation throughout the gradient, even in the thick areas, whereas the diffusion/interpenetration and subsequent immobilization of large proteins is partially hindered. This is crucial information in biosensor design that can be easily obtained from a gradient experiment on a single sample. Moreover, the partially hindered protein interpenetration, the marginal swelling upon hydration, and the unspecific nature of the graft polymerization suggest a matrix growth mechanism that favors the formation of a bushlike polymer structure with a certain degree of cross linking.

Introduction

Gradients are useful tools in studies of fundamental adsorption phenomena.[1−3] By means of a gradient, a single sample can reveal information that otherwise would require the investigation of a large number of homogeneous, single-property/composition samples. In addition, the occurrence of methodological errors during readout is minimized because gradients offer internal referencing. One can create gradients with respect to various properties, and relevant ones in biosensor applications are, for instance, density, composition, and presentation of immobilized biorecognition entities (receptors, antibodies etc.) as well as the extension or thickness of the sensing layer (matrix) on the supporting transducer substrate. The thickness is in many cases crucial because the matrix has to provide a nativelike environment for efficient ligand immobilization and biospecific binding to analyte molecules. It also has to be thick or dense enough to minimize contact with the underlying surface and thus prevent nonspecific binding (unless the substrate itself is protein-resistant). Poly(ethylene glycol) (PEG) in different forms has proven to be a suitable material for producing protein-resistant surfaces.[4−8] For that reason, PEG is a promising candidate when designing a biosensor matrix.[9−16] By generating a thickness gradient, the functionality of a sensing matrix can be investigated with respect to ligand penetration and immobilization and ultimately analyte binding. The present study, however, focuses exclusively on the initial steps of the biochip development process including matrix activation and ligand immobilization.

Surface gradients were first demonstrated in 1987 by Elwing et al.,[1] who created wettability gradients on silica substrates by a diffusion process involving dichlorodimethyl silane. Since then, gradients based on thiols on gold[2,17−19] and graft polymerization[20−23] have been developed. Recently, Wang et al.[21] demonstrated a gradient prepared electrochemically, where an inert thiol was gradually replaced by an initiator disulfide along the length of the sample. Subsequent grafting of poly(*N*-isopropylacrylamide) resulted in a thickness/density gradient. Zhao[20] reported on a method where two different initiator silanes were deposited on silica substrates in a gradient format by vapor diffusion and subsequent backfilling, followed by the two-step graft polymerization of methyl methacrylate and styrene. In a

* Corresponding author. E-mail: bolie@ifm.liu.se.

(1) Elwing, H.; Welin, S.; Askendal, A.; Nilsson, U.; Lundström, I. *J. Colloid Interface Sci.* **1987**, *119*, 203−210.
(2) Riepl, M.; Östblom, M.; Lundström, I.; Svensson, S. C. T.; Gon, A. W. D. v. d.; Schäferling, M.; Liedberg, B. *Langmuir* **2005**, *21*, 1042−1050.
(3) Gölander, C.-G.; Lin, Y.-S.; Hlady, V.; Andrade, J. D. *Colloids Surf.* **1990**, *49*, 289−302.
(4) Mori, Y.; Nagaoka, S.; Takiuchi, H.; Kikuchi, T.; Noguchi, N.; Tanzawa, H.; Noishiki, Y. *Trans. ASAIO* **1982**, *28*, 459−463.
(5) Desai, N. P.; Hubbell, J. A. *J. Biomed. Mater. Res.* **1991**, *25*, 829−843.
(6) Harris, J. M. *Poly(ethylene glycol) Chemistry: Biotechnical and Biomedical Applications*; Plenum Press: New York, 1992.
(7) Lee, J. H.; Jeong, B. J.; Lee, H. B. *J. Biomed. Mater. Res.* **1997**, *34*, 105−114.
(8) Zhang, M.; Desai, T.; Ferrari, M. *Biomaterials* **1998**, *19*, 953−960.
(9) Piehler, J.; Brecht, A.; Geckeler, K. E.; Gauglitz, G. *Biosens. Bioelectron.* **1996**, *11*, 579−590.
(10) Piehler, J.; Brecht, A.; Valiokas, R.; Liedberg, B.; Gauglitz, G. *Biosens. Bioelectron.* **2000**, *15*, 473−481.
(11) Huang, N.-P.; Vörös, J.; De Paul, S. M.; Textor, M.; Spencer, N. D. *Langmuir* **2002**, *18*, 220−230.
(12) Masson, J.-F.; Battaglia, T. M.; Kim, Y.-C.; Prakash, A.; Beaudoin, S.; Booksh, K. S. *Talanta* **2004**, *64*, 716−725.
(13) Muñoz, E. M.; Yu, H.; Hallock, J.; Edens, R. E.; Linhardt, R. J. *Anal. Biochem.* **2005**, *343*, 176−178.
(14) Uchida, K.; Otsuka, H.; Kaneko, M.; Kataoka, K.; Nagasaki, Y. *Anal. Chem.* **2005**, *77*, 1075−1080.
(15) Zhen, G.; Falconnet, D.; Kuennemann, E.; Vörös, J.; Spencer, N. D.; Textor, M.; Zürcher, S. *Adv. Funct. Mater.* **2006**, *16*, 243−251.
(16) Larsson, A.; Ekblad, T.; Andersson, O.; Liedberg, B. *Biomacromolecules* **2007**, *8*, 287−295.
(17) Liedberg, B.; Tengvall, P. *Langmuir* **1995**, *11*, 3821−3827.
(18) Terrill, R. H.; Balss, K. M.; Zhang, Y. M.; Bohn, P. W. *J. Am. Chem. Soc.* **2000**, *122*, 988−989.
(19) Morgenthaler, S.; Lee, S.; Zürcher, S.; Spencer, N. D. *Langmuir* **2003**, *19*, 10459−10462.
(20) Zhao, B. *Langmuir* **2004**, *20*, 11748−11755.
(21) Wang, X.; Tu, H.; Braun, P. V.; Bohn, P. W. *Langmuir* **2006**, *22*, 817−823.
(22) Bhat, R. R.; Tomlinson, M. R.; Genzer, J. *J. Polym. Sci., Part B: Polym. Phys.* **2005**, *43*, 3384−3394.
(23) Wu, T.; Efimenko, K.; Vlcek, P.; Subr, V.; Genzer, J. *Macromolecules* **2003**, *36*, 2448−2453.

10.1021/la700729q CCC: $37.00
Published on Web 09/27/2007

comparable approach, though restricted to one type of monomer, Wu et al.[23] graft polymerized acrylamide onto a gradient of initiator-functionalized silica substrates. Another similar study by Bhat et al.[22] described two orthogonal surface gradients where the density and the length of the polymer chains were varied. Again, silanization with initiators was used to start the graft polymerization.

Gradients that display a variation in the thickness or density of PEG-based building blocks have been reported previously.[7,24−26] In one case, PEG methacrylate monomers were graft polymerized at elevated temperatures onto polyethylene (PE) sheets with a varying degree of radio-frequency (rf) corona discharge activation, leading to the formation of a gradient.[7] Another report describes the immobilization of 5 kDa *N*-hydroxysuccinimide (NHS)−PEG onto amine-terminated self-assembled monolayers (SAMs) on gold, where the gradient was obtained by diffusion in an agarose gel.[25] In a third study, 2 kDa aldehyde-functionalized PEG was immobilized onto an amine-terminated silane gradient.[24] A fourth case worth mentioning in this context is a gradient of 2-hydroxyethyl methacrylate (HEMA) created by graft polymerization onto a gradient of an initiator-terminated silane deposited using a fluidic device.[26] These studies all focused on one or several of the following issues: adsorption of proteins and adhesion of platelets and cells. However, we are not aware of any earlier reports where a PEG-based matrix, in a gradient format, has been used to address critical issues regarding biochip design and development.

The aim of the present study is to introduce a novel methodology capable of producing a PEG-based matrix with varying thickness along a solid support. The gradient matrix is graft polymerized onto organic thin films using UV irradiation at 254 nm and a moving shutter that slowly uncovers the substrate, which offers spatially controlled irradiation and thereby a gradually increasing amount of grafted material—a thickness gradient. The present approach enables the production of gradients of varying thickness, 0−500 Å, and length, 5−20 mm, by adjusting the power of the UV lamp and the speed of the shutter. A hydroxyl-terminated PEG methacrylate monomer, with an average chain length of 10 ethylene glycol units ($PEG_{10}MA$), is graft copolymerized with a less complicated methacrylate monomer, HEMA, to yield the gradient. A range of different organic films have proven useful as grafting platforms.[27] To display such versatility in this respect, we employed two fundamentally different platforms, namely, a thin spin-coated cycloolefin polymer (COP) film and an ethylene glycol (EG)-terminated alkyl thiol self-assembled monolayer (SAM) on flat gold. The generated gradient facilitates the characterization of the matrix in terms of molecular diffusion and penetration of (i) a carboxylation agent suitable for the modification of hydroxyl terminals and the immobilization of (ii) two model proteins of different sizes and shapes. These events are studied with infrared reflection−absorption (RA) microscopy using a grazing-angle objective with a measuring spot size of ∼300 μm. The power of the present gradient approach is clearly demonstrated for this type of size exclusion experiment. For example, the relatively small carboxylation agent used offers homogeneous activation throughout the gradient, even in the thick areas, whereas the diffusion and interpenetration of large proteins is partially hindered. Partially hindered diffusion and immobilization of large proteins are discussed in terms of UV-initiated cross linking of the matrix and multipoint attachment of the proteins.

Biosensor matrixes based on PEG have been reported before,[9−15,28] though in a nongradient format, and in all of those cases, linear PEG chains were end-point attached to the surface, thus providing, at maximum, one functional group per grafting site (PEG chain) for immobilization. Such a design has the inherited disadvantage that it limits the number of available immobilization sites for the ligand and thereby the attainable response upon binding to the analyte. The presented PEG matrix, however, has the potential of providing a large number of functional groups (e.g., COOH) per grafting site and thereby an increased response (given that it is permeable to the molecules of interest). Furthermore, the wide range of organic substrates that can be used as grafting platforms and the lack of need for polymerization initiators make this approach very attractive and versatile. In addition, the nature of the technique makes it suitable for pattering applications, which will be reported elsewhere.

Experimental Section

Sample Preparation. Gold-coated silicon (100) wafers (Siltronic AG, Germany) with a native oxide layer (∼20 Å thick) were used as substrates in all experiments. In the cases where a polymer film was used as the graft polymerization platform, the wafers were cut into 9 × 27.5 mm^2 pieces and coated with 25 Å of titanium (Balzers, Liechtenstein, 99.9%) and 2000 Å of gold (Nordic High Vacuum AB, Kullavik, Sweden, 99.99%) by electron beam evaporation using a Balzers UMS 500 P system. The evaporation rates were 1 and 10 Å/s for titanium and gold, respectively. The base pressure was at least 10^{-9} mbar, and the pressure during evaporation was on the low 10^{-7} mbar scale. The substrates were ultrasonicated in 99.5% ethanol (Kemetyl, Haninge, Sweden) for 5 min and rf plasma treated at 200 W for 1 min prior to deposition of the polymer film.[16] For thiol-based graft polymerization, the silicon wafers were scored in a 12.5 × 12.5 mm^2 grid pattern and then metallized in a custom-made resistive evaporation system. The wafers were coated with 25 Å of chromium (Balzers, 99.9%) and 2000 Å of gold. The evaporation rates were 1 and 10 Å/s for chromium and gold, respectively. The base pressure was on the low 10^{-6} mbar scale, and the pressure during evaporation was on the high 10^{-6} mbar scale. Before use, the coated wafers were cut along the score lines and cleaned in a 5:1:1 mixture of Milli-Q water (Milli-Q, Millipore), 30% hydrogen peroxide (Merck KGaA, Germany), and 25% ammonia (Merck KGaA) for 10 min at 85 °C (TL-1 procedure).

The general grafting procedure is described elsewhere in detail,[16] and only a short description is given here. It should be noted, however, that the previous work exclusively covered an approach where the grafting platform consisted of a thin layer of a COP deposited by spin coating, whereas in this article a thiol SAM was used as well. In the latter case, the gold substrates were incubated in 100 μM $HS(CH_2)_{11}CONH(C_2H_4O)_{11}CH_3$ (HS−UDA−$mPEG_{10}$) (Polypure AS, Norway) in 99.5% ethanol for at least 24 h at room temperature. The samples were then rinsed twice in 99.5% ethanol, ultrasonicated for 3 min, rinsed twice more in 99.5% ethanol, and subsequently dried in a nitrogen flow. Thereafter, a drop of monomer solution was placed on the underside of a clean quartz disk, which was brought into contact with the substrate to form a sandwich assembly in which the sample became freely hanging, and was kept in place by the surface tension of the liquid (Figure 1A). All gradients were grafted using an aqueous 1:1 monomer mixture of $PEG_{10}MA$ and HEMA (both from Sigma-Aldrich Sweden AB) at a total concentration of

(24) Lin, Y. S.; Hlady, V.; Gölander, C.-G. *Colloids Surf., B* **1994**, *3*, 49−62.
(25) Mougin, K.; Ham, A. S.; Lawrence, M. B.; Fernandez, E. J.; Hillier, A. C. *Langmuir* **2005**, *21*, 4809−4812.
(26) Mei, Y.; Wu, T.; Xu, C.; Langenbach, K. J.; Elliott, J. T.; Vogt, B. D.; Beers, K. L.; Amis, E. J.; Washburn, N. R. *Langmuir* **2005**, *21*, 12309−12314.
(27) Within our group, thiols $HS(CH_2)_{16}OH$, $HS(CH_2)_{15}COOH$, $HS(CH_2)_{11}CONH(C_2H_4O)_{11}CH_3$, $HS(CH_2)_2(C_2H_4O)_6OCH_3$, and $HS(CH_2)_{15}CONH(C_2H_4O)_4(CH_2)_2NHCOCH_2C_6H_3(NO_2)_2$ on gold and silanes (3-aminopropyl)triethoxysilane and 3-methacryloxypropyltrimethoxysilane on silica and glass have been used as grafting platforms. In addition, the plastic polymers polyethylene, poly(methyl methacrylate), cycloolefin polymer, and polystyrene have been used as self-supported platforms. The latter two have also been used as spin-coated films on gold, silica, and glass.

(28) Lata, S.; Piehler, J. *Anal. Chem.* **2005**, *77*, 1096−1105.

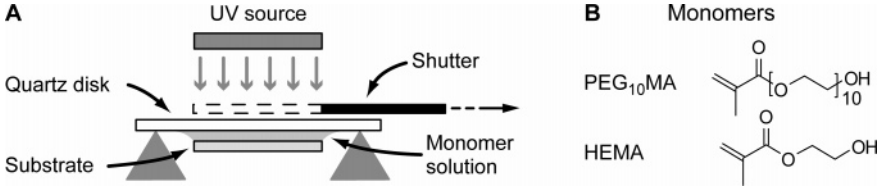

Figure 1. (A) Graphic displaying the sandwich assembly used during grafting as well as the shutter that enables the formation of the gradient. (B) Chemical structures of the two methacrylate monomers used in the graft polymerization process.

240 mM (Figure 1B). The assembly was placed on supports in a reaction chamber, which was purged with nitrogen gas for 1 min before and throughout the grafting event. In the case of the COP platform, the light source employed to initiate the graft polymerization was a Newport Apex light source with a 100 W Hg lamp, and that for the SAM platform was a Philips TUV PL-L 18 W Hg lamp. The Apex unit provided collimated output and was used along with a dichroic mirror with its main reflectivity at 240−255 nm, while the irradiation of the Philips lamp was noncollimated but had a distinct emission peak at 254 nm. Because the present polymerization process is sustained by a fairly low irradiation power, it is relatively gentle to the different experimental components (e.g., the supporting SAM). Infrared and ellipsometric data confirm that degradation is limited to the tail group of a typical SAM and the thickness decrease is around 10% after 10 min of irradiation from the 18 W Hg UV source (in the absence of monomers in the solution). Reports on the intentional stripping of alkyl thiol SAMs using Hg lamps are generally carried out in air and employ considerably higher power and longer exposure times compared to the present experimental parameters. For instance, a crude estimate gives a UV dose that is at least 2 orders of magnitude lower than that used by Hemminger and co-workers.[29] During the grafting process a shutter, placed above the sandwich assembly, slowly uncovered the substrate, resulting in an exposure gradient (Figure 1A). The shutter was moved at constant speeds of 2.85 and 1.90 mm/min for the COP- and SAM-based platforms, respectively. The matrixes were then carboxylated using bromoacetic acid.[30] After 20 min of activation of the carboxyl groups with an aqueous mixture of *N*-ethyl-*N*′-[3-(dimethylamino)-propyl]-carbodiimide (EDC) (Biacore AB, Uppsala, Sweden) and NHS (Sigma-Aldrich Sweden AB) at 0.2 and 0.05 M, respectively, two different proteins were immobilized via their lysine residues during 60 min of incubation in 10 mM sodium acetate buffer, pH 4.5. The proteins were human serum albumin (HSA) (Sigma-Aldrich Sweden AB) MW 66 kDa, pI 4.9[31] and human fibrinogen (HFib) (Hyphen BioMed SAS, France) MW 340 kDa, pI 5.8,[31] both at a concentration of 700 nM. These two proteins were selected because of their differences in size and shape. However, we have successfully immobilized a range of proteins (lysozyme, streptavidin, avidin, protein A, anti-β-2-microglobulin) in nongradient matrixes prepared under identical conditions to those employed here. By choosing a solution with a low ionic strength and a pH lower than the pI of the proteins (pH 4.5), they will be electrostatically attracted to the matrix, which is expected to be negatively charged at that pH.[30] Once inside the matrix, the proteins are able to bind covalently to the activated carboxyl groups. It should be stressed, however, that no attempts were made to optimize the pH used during immobilization.

Null Ellipsometry. The ellipsometric thickness was determined using a Nanofilm EP^3-SE imaging ellipsometer operating in the one zone nulling mode. The angle of incidence was set at 60°, and the wavelength was 831 nm. A 2× magnification objective was used, and the refractive index of the PEG matrix in the dry state was assumed to be 1.5. The distance between the measuring points was 635 μm, and the measuring spot was 300 × 300 μm^2. A motorized sample table facilitated measurements along the gradient. The background refractive index was recorded from an HS−UDA−mPEG$_{10}$ SAM on gold.

Infrared Spectroscopy. A Bruker Hyperion 3000 microscope connected to a Bruker Tensor 27 system was utilized to record the infrared RA spectra. The detector was a liquid-nitrogen-cooled mercury cadmium telluride (MCT) detector and the grazing angle objective, allowing two surface reflections, had a set of angles of incidence ranging from 52 to 83°. Because a circular beam of radiation at nonzero angles of incidence results in an elliptical area of reflection, the measuring spot will be elliptical when using a grazing angle objective. During the presented experiments, the minor axis of the ellipse (which is perpendicular to the plane of incidence) was aligned parallel to the direction of the gradient. It was determined that an ellipse with a minor axis of 300 μm covers 95% of the recorded absorption intensity whereas the distances between the measuring points were 1000 and 635 μm for the COP and the SAM platform, respectively. A motorized sample table facilitated measurements along the gradient. Being aligned perpendicular to the direction of the gradient, the enlargement of the measuring spot due to the major axis posed no problem. To minimize the presence of gaseous water in the measurement chamber, it was purged with dry nitrogen gas. At each measuring spot, 800 scans were collected at a resolution of 4 cm^{-1}. A three-term Blackman Harris apodization function was applied to the interferograms prior to Fourier transformation. All RA spectra were baseline corrected using a concave rubber band method with 64 points and 10 iterations. A deuterated hexadecanethiol ($HS(CD_2)_{15}CD_3$) SAM on gold was used to record the background spectra.

Results and Discussion

Poly(ethylene glycol)-based gradients have been investigated before, using IR spectroscopy operating in the attenuated total reflection (ATR) mode.[32] In that case, each spectrum was obtained by averaging over a 1 cm segment (after having cut the sample into pieces) along a 5-cm-long gradient. This approach offers poor lateral resolution, and it does not invite further surface modifications and subsequent measurements. The use of an infrared microscope with a grazing angle objective offers the possibility of examining small areas, and an accurate motorized sample table ensures equidistant movements between measuring spots. Figure 2A,B shows the evolution of the infrared intensities along a 20 mm nonmodified PEG-based gradient on a COP-coated gold substrate. As expected, the peak intensities increase monotonically with increasing matrix thickness. Most of the peaks have been assigned previously,[16] but a few peaks are of particular interest here. The ester carbonyl C═O, adjacent to the backbone of the formed polymer, is clearly seen at 1732 cm^{-1}, and the integral of this peak can be correlated to the ellipsometric thickness of the matrix (see below) because each monomer (building block) contains one ester group. Figure 2C,D display data from a 7-mm-long gradient on a SAM after carboxylation and subsequent immobilization of HFib, respectively. In Figure 2C, the presence of the carboxylate groups is seen as asymmetric stretches at 1609 and ∼1585 cm^{-1}, respectively, which suggests

(29) Huang, J.; Dahlgren, D. A.; Hemminger, J. C. *Langmuir* **1994**, *10*, 626−628.

(30) Löfås, S.; Johnsson, B. *J. Chem. Soc., Chem. Commun.* **1990**, 1526−1528.

(31) Fasman, G. D., Ed. *Handbook of Biochemistry*; CRC Press: Cleveland, OH, 1976; Vol. II, Section A (Proteins).

(32) Jeong, B. J.; Lee, J. H.; Lee, H. B. *J. Colloid Interface Sci.* **1996**, *178*, 757−763.

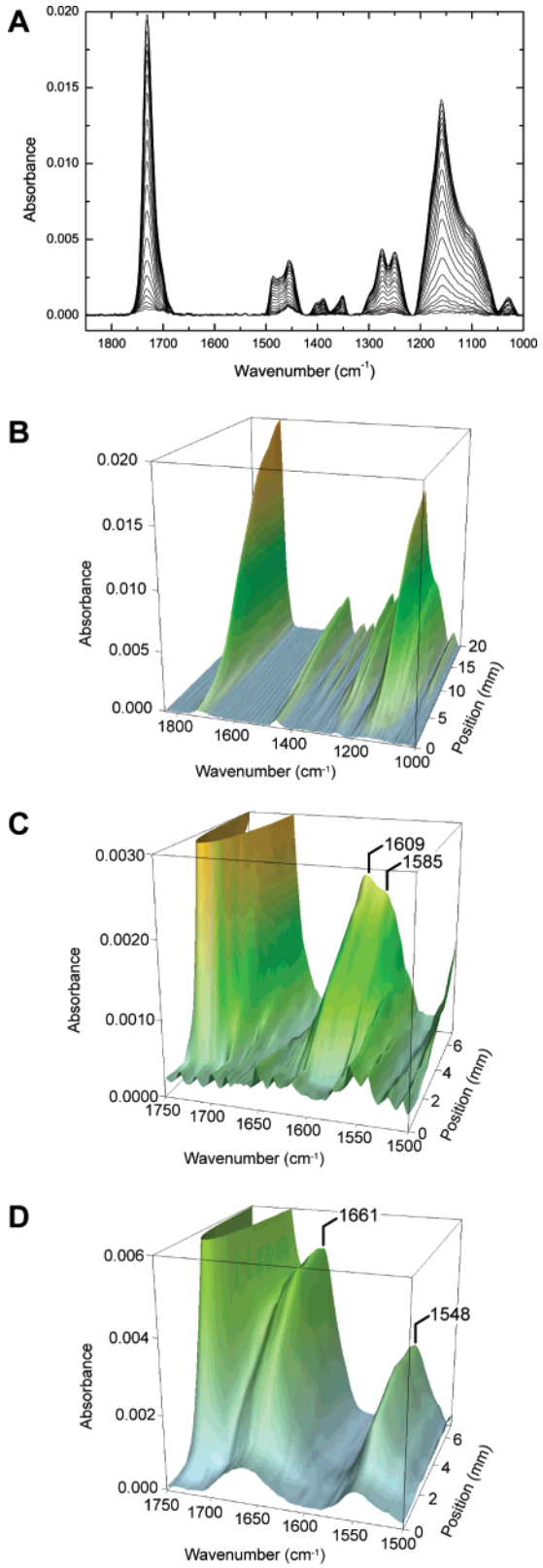

Figure 2. Infrared spectra from RA measurements on PEG-based graft-polymerized matrixes. (A) Spectra from a nonmodified, 20-mm-long gradient on a COP film. (B) Spatially resolved 3D plot of the same data as in A. (C) 3D plot of a carboxylated, 7-mm-long matrix gradient on a SAM. (D) 3D plot of a SAM with a 7-mm-long matrix gradient with immobilized HFib. For additional spectra, see Supporting Information.

that the matrix has been successfully carboxylated. The 1609 cm^{-1} peak is attributed to the carboxylate group introduced on the HEMA tail, whereas the 1585 cm^{-1} shoulder stems from the carboxylate on the longer $PEG_{10}MA$ tail. The immobilized HFib is seen as two distinct peaks, Amide I and II, at 1661 and 1548 cm^{-1}, respectively, in Figure 2D. The presence of the supporting SAM can be confirmed by the peaks that correspond to helical (1345 and 1115 cm^{-1}) and all-trans (1146 cm^{-1}) conformers[33] of the EG segments in the HS−UDA−$mPEG_{10}$ molecule (Supporting Information).

The thickness of the matrix is an important design parameter that can be determined using ellipsometry. Lin et al.[24] reported on a PEG-based gradient with a maximum thickness of 11 Å, while Mougin et al.[25] reached a maximum thickness of 160 Å. Both of these gradients spanned over similar distances (∼7 mm) as for the gradients on SAMs described herein. In Figure 3A, the dry-state gradient thickness is plotted against the integral values of the C═O peak. As seen, the thickness varies between 0 and ∼500 Å. The nearly linear relation between the ellipsometry thickness and the integral C═O values suggests that the graph can be used to estimate the thickness from IR intensity data obtained at any position along a gradient. Figure 3B shows the integral values of the COO^- peak along with those of the C═O peak as a function of position along the gradient. It is evident that the carboxylation process is efficient even in the thickest parts of the matrix. The fact that COO^- integral values still increase with increasing thickness, even at high thickness, indicates that the carboxylation agent (bromoacetic acid) is not excluded because of steric constraints. Corresponding comparisons between the amide II integral values and those of the C═O peak from the spectra of immobilized HSA and HFib (cf. Figure 2D) are shown in Figure 3C,D, respectively. To avoid the contribution of the succinimidyl carbonyl group at 1742 cm^{-1}[34] (which appears when subtracting the spectrum of a carboxylated matrix from that of an EDC/NHS activated matrix), the carbonyl integral values are taken from the spectra recorded prior to EDC/NHS activation. By analogy to the case of carboxylation, HSA does not seem to be sterically blocked, although it is seemingly hindered, from reaching the thickest parts of the matrix. Human serum albumin is a heart-shaped protein with approximate dimensions of 80 × 80 × 30 $Å^3$.[35] It is clear, however, that HSA, being a lot larger than the carboxylation agent, penetrates the matrix less efficiently. It should be remembered, though, that the incubation time is 16 times longer and the concentration is more than 6 orders of magnitude higher in the carboxylation process compared to the one used in the protein immobilization experiments. In other words, it might be possible to reach a more even distribution of proteins in the matrix by prolonging the immobilization time and/or increasing the HSA concentration, provided that protein-mediated cross linking can be avoided. (See below.) We found, however, that an extension of the immobilization time of HSA, from 1 to 16 h, had a marginal effect on the total amount of immobilized protein. The amide II integral values in Figure 3D reveal that the amount of immobilized HFib levels off at some point in the range of 3−3.5 mm, which corresponds to a C═O integral value of ∼0.25. When consulting Figure 3A, this value corresponds to a dry-state thickness of the matrix of ∼200 Å. This thickness should be regarded as an approximate penetration limit for HFib during immobilization under the present circumstances. In contrast to HSA, the larger HFib seems to be blocked from penetrating the matrix any deeper than this. It should be noted that the higher pI of HFib, compared to that of HSA, is actually more favorable from an immobilization

(33) Valiokas, R.; Svedhem, S.; Svensson, S. C. T.; Liedberg, B. *Langmuir* **1999**, *15*, 3390−3394.
(34) Dordi, B.; Schönherr, H.; Vancso, G. J. *Langmuir* **2003**, *19*, 5780−5786.
(35) Sugio, S.; Kashima, A.; Mochizuki, S.; Noda, M.; Kobayashi, K. *Protein Eng.* **1999**, *12*, 439−446.

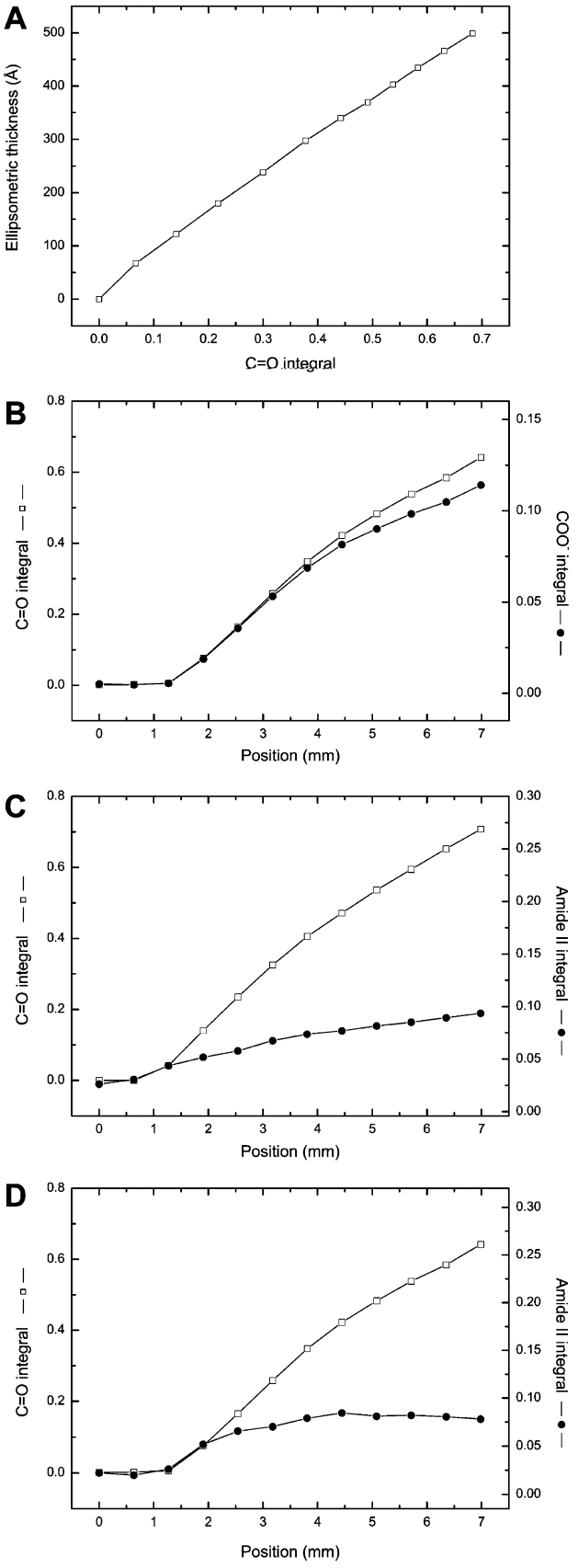

Figure 3. (A) Relation between C═O integral values and the ellipsometric thickness of a carboxylated matrix gradient in its dry state on a SAM platform. (B) Comparison between C═O and COO^- integral values from a carboxylated matrix gradient on a SAM platform. (C, D) Comparison between C═O (recorded prior to EDC/NHS activation) and amide II integral values (recorded after protein immobilization: (C) HSA and (D) HFib).

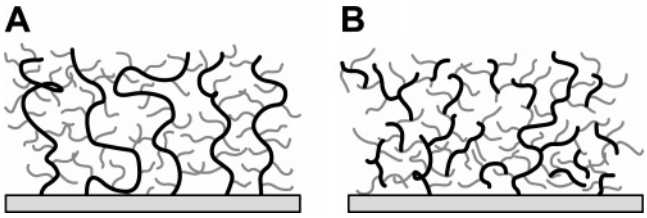

Figure 4. Two conceivable models to describe the resulting matrix after graft polymerization. (A) Free radicals are formed exclusively on the organic platform and react exclusively with the ethenyl groups of the monomers, leading to surface-anchored linear backbones with protruding PEG arms. (B) Free radicals are formed not only on the platform but also on different parts of the matrix itself, leading to a more bushlike structure.

perspective because of the increased electrostatic attraction. Therefore, it seems that HFib is too large to penetrate the pores in the matrix. The length of HFib is 475 ± 25 Å, and it contains three nodes with diameters of 50−60 Å, which are linearly connected by rods with diameters of 8−15 Å.[36] Such a large protein can also interact more strongly with the matrix by forming multiple attachment points. Multipoint attachment is, in fact, a very likely scenario considering the extremely large number of carboxylic acid groups introduced during activation in bromoacetic acid.[16] Taken together, it seems reasonable to assume that the matrix is cross linked upon formation as well as during the immobilization of HFib (and perhaps also HSA), which effectively blocks additional proteins from reaching the thicker regions of the matrix.

The differences in penetration depth raise questions concerning details of the matrix structure. Figure 4 depicts two different structural models of the resulting matrix. In the case seen in Figure 4A, the reaction starts exclusively from sites on the organic surface by the formation of free radicals upon UV exposure. The free radicals then interact with the unsaturated terminals (ethenyl groups) of the monomers, whereby a bond is created along with the formation of a new free radical, which in turn can react with yet another monomer and so on. This phenomenon is known as living polymerization. Upon free radical formation on the surface, free radicals may also be released into the solution, giving rise to non-surface-bound polymer chains (which may fuse with surface-bound chains). The result would be linear polymer chains anchored at the platform and non-anchored chains, which later could be washed away. We find this scenario rather improbable considering the fact that no specific initiators are needed to start the graft polymerization process. Thus, the grafting process appears not to be surface-specific. Instead, it seems that the UV light is aggressive enough to create free radicals quite unspecifically, thus initiating graft polymerization reactions not only on the surface but also on the already created matrix and on free monomers (Figure 4B). We find that the structure proposed in Figure 4B is very plausible because the grafting process works on a number of different organic platforms such as polymers and alkane thiol and silane SAMs with different tail groups, including EG segments. Of course, the different types of platforms/chemistries display a varying degree of grafting efficiency, but the process works very well in many cases.[27]

There are other studies that describe self-initiated photografting under UV irradiation at 254 nm on nonactivated substrates such

(36) Hall, C. E.; Slayter, H. S. *J. Cell Biol.* **1959**, *5*, 11−27.

as poly(ethylene terephthalate)[37] and PE[38] using different methacrylates, including both PEG_xMA and HEMA. Wang and Brown[38] discussed two possibilities of photoinduced graft polymerization: (i) the monomers themselves form free radicals that can interact with the substrate (and other monomers) and (ii) excitation of the monomers to triplet states, capable of abstracting hydrogen from the substrate (and other monomers) under the formation of free radicals, which may then react with monomers in solution. In a somewhat related study, Stachowiak et al.[39] also present ideas along these lines. Therefore, it seems reasonable to conclude that the free radical formation is indeed quite unspecific. Such a growth process would lead to a more bushlike structure with a considerable number of cross-linked and branched segments. In addition, atomic force microscopy measurements reveal a swelling of ∼30% upon hydration for a matrix with a dry thickness of about 370 Å (data not shown). Because this is relatively small swelling, the model in Figure 4B is further favored. Of course, one can also argue that the branching and subsequent cross linking vary during the course of the grafting process and that the structure shown in Figure 4A is dominant during the initial phase but that the number of branched and cross-linked chains, as in Figure 4B, increases with increasing thickness. A matrix containing considerable numbers of structurally different chains (as a consequence of branching and/or cross linking) would most likely display an altered IR signature as compared to a matrix composed of end-point-grafted chains as in Figure 4A. However, IR spectra recorded from thin and thick parts of the sample are indistinguishable (except for lower absolute intensity and a higher noise level in the "thin" spectrum, see Supporting Information). Thus, it seems that the structural variations between the thin and thick regions of the gradient matrix are very small or negligible.

In summary, the second model shown in Figure 4B is very plausible, although it should be regarded as tentative. In effect, the limited permeability will prevent the proteins, HFib in particular, from freely diffusing into the matrix and attaching homogenously to the activated COOH groups. More work is obviously required to obtain a comprehensive understanding of the structural and functional properties of the matrix, and such studies are underway. Of key importance is to develop protocols that enable the growth of less compact matrixes, similar to those prepared using living polymerization (Figure 4A) because a flexible and fully permeable matrix is crucial for obtaining high-quality kinetic and quantitative data from a biosensing experiment.[40,41] However, a less dense matrix may expose the underlying substrate, which therefore has to be designed with care to avoid nonspecific binding. Alternative chemical strategies to control the growth and density of the matrix, including surface-anchored initiators/inhibitors, inert porogens, and/or bulky polymeric additives, are definitely worthwhile for exploring that purpose. We hope that such an approach would result in more linear, less dense polymer architecture as schematically outlined in Figure 4A. In another interesting approach that was employed by Arenkov et al.,[42] the porosity of a polyacrylamide gel was increased by copolymerization with *N,N′*-(1,2-dihydroxyethylene) bisacrylamide, which is a cross linker that may be cleaved afterward. Moreover, to reduce the risk of cross linking due to the formation of multiple bonds between the matrix and the immobilized protein, one could envision employing smaller recognition molecules, such as antibody Fab fragments, minimum-recognition sequences using peptides,[43] and even non-natural receptors based on polypeptide scaffolds.[44]

Conclusions

A novel method of producing a PEG-based gradient for use in biochip and biosensor applications is demonstrated. The matrix is generated from methacrylate monomers under UV irradiation at 254 nm. Compared to previous reports on PEG-containing biosensor surfaces, which are exclusively based on nonbranched PEG chains, thus providing a maximum of one immobilization point per grafting site, our approach offers the potential of a higher density of immobilization points and thereby a larger response during analyte binding. Furthermore, the process supports the use of a wide range of substrates and lacks the need for dedicated initiators, making it very versatile and compatible with the broad range of transducer materials used in the biosensing community. The nature of this approach makes it suitable for patterning, which provides opportunities for the production of microarrays. The use of the present approach for patterning applications will be reported elsewhere.

Thickness gradients are useful model coatings for characterizing the diffusion and penetration of molecular species into biosensing matrixes. Infrared microscopy in combination with a grazing angle objective is demonstrated to be a powerful method for the characterization of such gradients at high lateral resolution. Note that the measuring spot size used in this initial work was ∼300 μm, a size that is far away from the diffraction limit of the IR microscopy setup (∼10 μm). Given the signal-to-noise ratio in the recorded spectra, it should be possible to decrease the size of the spot even further and thereby improve the lateral resolution.

The length of the present gradient is easily tuned by altering the speed of the shutter, and the maximum thickness is governed by the total irradiation time and power. The collimated light source used naturally gives better control over the starting and ending positions of the gradient, although a non-collimated source is sufficient in most cases.

A comparison between carboxylation and protein immobilization data indicates that the proteins are sterically hindered from penetrating the thick parts of the matrix. It is found that HFib penetrates the matrix down to a depth of ∼200 Å, whereas no such sharp penetration limit could be found for HSA. Three factors that might cause this behavior are discussed: (i) a matrix that is too dense as a result of a high grafting density, (ii) a cross-linked matrix, and (iii) the presence of multiple attachment points between the matrix and the proteins. The latter also results in cross linking, thereby opposing the penetration of additional proteins. Taken together, it seems as if the matrix adopts a bushlike structure with an undefined number of cross-linked polymer chains. More effort is clearly needed to elucidate the true nature of the matrix. For instance, the production of less-dense matrixes may be possible by including cleavable cross linkers, inert porogens, and/or other additives in the monomer solution during graft polymerization. In kinetic applications, for example, it is crucial that the analyte can diffuse freely into and out of the

(37) Uchida, E.; Uyama, Y.; Ikada, Y. *Langmuir* **1994**, *10*, 481−485.
(38) Wang, H.; Brown, H. R. *Macromol. Rapid Commun.* **2004**, *25*, 1095−1099.
(39) Stachowiak, T. B.; Svec, F.; Frechet, J. M. J. *Chem. Mater.* **2006**, *18*, 5950−5957.
(40) Myszka, D. G.; Morton, T. A.; Doyle, M. L.; Chaiken, I. M. *Biophys. Chem.* **1997**, *64*, 127−137.
(41) Fong, C.-C.; Wong, M.-S.; Fong, W.-F.; Yang, M. *Anal. Chim. Acta* **2002**, *456*, 201−208.
(42) Arenkov, P.; Kukhtin, A.; Gemmell, A.; Voloshchuk, S.; Chupeeva, V.; Mirzabekov, A. *Anal. Biochem.* **2000**, *278*, 123−131.
(43) Laricchia Robbio, L.; Liedberg, B.; Platou Vikinge, T.; Rovero, P.; Beffy, P.; Revoltella, R. P. *Hybridoma* **1996**, *15*, 343−350.
(44) Enander, K.; Dolphin, G. T.; Liedberg, B.; Lundström, I.; Baltzer, L. *Chem.−Eur. J.* **2004**, *10*, 2375−2385.

matrix. It is also essential to keep the number of immobilized ligands and therefore the number of introduced COOH groups, at a low level in order to avoid mass transport limitations. Thus, the carboxylation protocol needs to be fine tuned for the extraction of reliable kinetic data. A complementary approach to carboxylation using bromoacetic acid could be to use precarboxylated monomers, whereby the number of carboxyl groups could be adjusted more accurately. It should be emphasized, however, that the problems associated with a too dense matrix can be turned into an advantage when one would like to prevent large macromolecular and cellular components from entering the sensing matrix (a sort of size-selective filter), for example, for detection of low molecular weight compounds.

Acknowledgment. This work was supported by the Swedish Research Council (VR) and the Foundation for Strategic Research (SSF) through the Biomimetic Materials Science Program.

Supporting Information Available: Infrared spectra of the gradients in the fingerprint region. This material is available free of charge via the Internet at http://pubs.acs.org.

LA700729Q